

Applications of Mathematics

Pengzhan Huang; Qiuyu Zhang

A recovery-based a posteriori error estimator for the generalized Stokes problem

Applications of Mathematics, Vol. 65 (2020), No. 1, 23–41

Persistent URL: <http://dml.cz/dmlcz/147993>

Terms of use:

© Institute of Mathematics AS CR, 2020

Institute of Mathematics of the Czech Academy of Sciences provides access to digitized documents strictly for personal use. Each copy of any part of this document must contain these *Terms of use*.



This document has been digitized, optimized for electronic delivery and stamped with digital signature within the project *DML-CZ: The Czech Digital Mathematics Library* <http://dml.cz>

A RECOVERY-BASED A POSTERIORI ERROR ESTIMATOR FOR
THE GENERALIZED STOKES PROBLEM

PENGZHAN HUANG, Urumqi, QIUYU ZHANG, Wuhan

Received November 15, 2018. Published online January 9, 2020.

Abstract. A recovery-based a posteriori error estimator for the generalized Stokes problem is established based on the stabilized $P_1 - P_0$ (linear/constant) finite element method. The reliability and efficiency of the error estimator are shown. Through theoretical analysis and numerical tests, it is revealed that the estimator is useful and efficient for the generalized Stokes problem.

Keywords: generalized Stokes problem; recovery-based error estimator; adaptive method; finite element method

MSC 2010: 65N30, 65N50

1. INTRODUCTION

Let Ω be a bounded and polygonal domain with Lipschitz continuous boundary $\partial\Omega$. We consider the generalized Stokes problem (GSP) as follows: Find (u, p) such that

$$(1.1) \quad \begin{cases} \sigma u - \nu \Delta u + \nabla p = f & \text{in } \Omega, \\ \operatorname{div} u = 0 & \text{in } \Omega, \\ u = 0 & \text{on } \partial\Omega, \end{cases}$$

where $u = u(x) = (u_1(x), u_2(x))^\top$ denotes the velocity vector, $p = p(x)$ is the pressure, $f = f(x) = (f_1(x), f_2(x))^\top$ is a given source-like function, and ν and $\sigma \geq 1$ represent the coefficient of viscosity and reaction, respectively. The GSP can be seen as a vital substep of an unsteady equation or other non-linear equations, such as non-Newtonian flows, Navier-Stokes equations, convection-dominated convection-diffusion problems and so on.

The research has been supported by the NSF of China (grant number 11861067).

At the time of writing, there are numerous works devoted to the development of efficient methods for the GSP, such as finite element method, finite difference method, radial basis function, spectral method and so on. Bustinza et al. have studied a low-order mixed finite element for this problem [9]. A local stabilized nonconforming finite element method for the GSP was proposed by Wang et al. [28]. Larin and Reusken compare a coupled multigrid method with Braess-Sarazin and Vanka-type smoothers [20]. Deng and Feng [14] develop and analyze the multigrid methods based on mixed element methods for the generalized Stokes equations. An unusual stabilized finite method is presented and analyzed for GSP with a dominating zeroth order term by Barrenechea and Valentin [4]. Bank and Welfert show a comparison between the mini-element and Petrov-Galerkin formulations [3]. A covolume or MAC-like method is introduced for approximating the GSP by Chou [13]. Burman and Hansbo use a continuous interior penalty method to research edge stabilization of GSP in [8]. Alternatively, Nafa and Wathen analyze pressure stabilized finite element methods for solving the solution of the GSP and investigate their stability and convergence properties [21]. An augmented mixed formulation is applied to GSP which is obtained adding suitable least squares terms to the corresponding velocity-pseudostress formulation of the GSP [5].

Nowadays, it is very popular to apply adaptive methods to save computer time and it has been proved that it is useful and efficient in scientific computing [2], [16], [17], [26], [29], [18]. A posteriori error estimate for the $P_1 - P_0$ stabilized finite element methods has been studied by Kay and Silverste [19]. Two a posteriori error estimators for the mini-element discretization of Stokes equations have been presented by Verfürth [25], involving the residual estimator. For the considered problem based on residual a posteriori error estimator, Repin and Stenberg have derived estimates by transforming the basic integral identity defining a generalized solution to GSP and proved a posteriori estimates for the velocity field based on the difference between exact and approximate pressure function in the L^2 -norm [22]. Besides, Araya et al. have presented an adaptive strategy (based on an a posteriori error estimator) for a stabilized finite element method [1].

As for the recovery-based a posteriori error estimator, it was first introduced by Zienkiewicz and Zhu [31], [32]. Further, the recovery-based error estimator is analyzed for the Poisson equation based on the lowest order finite element approximation by Rodríguez [23] and Carstensen [10]. For the Stokes equations, Carstensen and Funken have shown the recovery-based a posteriori error estimator for the nonconforming finite element approximation [11]. Moreover, Song et al. [24] propose a recovery-based error estimator for the stabilized $P_1 - P_0$ finite element approximations, and apply the so-called projection stabilized method [30], i.e., add the

difference of the numerical pressure and its projection onto the continuous piecewise linear finite element space.

In this paper we will present a posteriori error analysis of a stabilized method for the GSP with a recovery-based estimator, and through theoretical analysis and numerical experiments we will see that the estimator is useful and efficient for the GSP. The present paper is organized as follows. In Section 2, we introduce a stabilized finite element method for the GSP. In Section 3, we propose a recovery-based estimator and analyze its reliability and efficiency. In the last section, we numerically confirm the theoretical results.

2. STABILIZED $P_1 - P_0$ FINITE ELEMENT APPROXIMATION

In this section, we need to introduce the following Hilbert spaces to establish the weak form:

$$X = H_0^1(\Omega)^2, \quad M = L_0^2(\Omega) = \left\{ q \in L^2(\Omega) : \int_{\Omega} q \, dx = 0 \right\}.$$

Next, let $B((u, p), (v, q)) = \sigma(u, v) + \nu(\nabla u, \nabla v) - (p, \operatorname{div} v) + (q, \operatorname{div} u)$ and $f(v) = (f, v)$. Then a weak solution of system (1.1) can be defined as follows: Find $(u, p) \in X \times M$ such that

$$(2.1) \quad B((u, p), (v, q)) = f(v) \quad \forall (v, q) \in X \times M.$$

It is easy to verify that the bilinear form $B((\cdot, \cdot), (\cdot, \cdot))$ satisfies the inf-sup condition which ensures the uniqueness of (2.1), i.e., for all $(v, q) \in X \times M$ there exists a positive constant β_1 such that [28]

$$\inf_{(u, p) \in X \times M} \sup_{(v, q) \in X \times M} \frac{B((u, p), (v, q))}{\|(u, p)\| \|(v, q)\|} \geq \beta_1,$$

where the energy norm $\|\cdot\|$ is defined by $\|(v, q)\| = (\|v\|_1^2 + \|q\|^2)^{1/2}$.

Further, let $\tau_h = \{T\}$ be a triangulation of the domain $\overline{\Omega}$ with the mesh parameter $h = \max_{T \in \tau_h} \{\operatorname{diam}(T)\}$. Assume the triangulation τ_h is regular; i.e., the ratio h_T/ϱ_T is bounded by a constant C which is independent of h . Here, h_T denotes the longest edge of T and ϱ_T the diameter of the largest circle inscribed in T .

Let R_1 be the space consisting of continuous functions which are linear on each triangle, i.e.,

$$R_1 = \{v_h \in C^0(\overline{\Omega}) : v_h|_T \in P_1(T) \quad \forall T \in \tau_h\},$$

where $P_1(T)$ is the space of linear polynomials on the element T . Besides, we need the piecewise constant finite element space

$$R_0 = \{q_h \in L^2(\Omega): q_h|_T \in P_0(T) \forall T \in \tau_h\},$$

where $P_0(T)$ are the constant polynomials on the element T .

In this paper, we will apply the stabilized mixed method for solving the GSP based on the lowest conforming pair

$$X_h = X \cap R_1^2,$$

and

$$M_h = M \cap R_0.$$

It is known that the lowest conforming pair does not satisfy the inf-sup condition, therefore some stabilized mixed methods are used for the lowest conforming pair. This paper is focused on the projection stabilized method in [7], which does not require side based data structures and is parameter free. The stabilization term is given by

$$S(p_h, q_h) = (p_h - \Pi p_h, q_h - \Pi q_h) \quad \forall p_h, q_h \in M_h,$$

where Π is defined by $\Pi: L^2(\Omega) \rightarrow R_1$ and has the following properties [7], [24]:

$$\begin{aligned} C\|[p_h]_e\|_{S_h} &\leq \|p_h - \Pi p_h\| \leq C\|[p_h]_e\|_{S_h} \quad \forall p_h \in R_0, \\ \|p_h - \Pi p_h\| &\leq C\|p_h\| \quad \forall p_h \in R_0. \end{aligned}$$

Here S_h denotes the set of all interior sides in Ω , $e \in S_h$ is an edge and the norm is

$$\|v\|_{S_h} = \left(\sum_{e \in S_h} h_e \|v\|_e^2 \right)^{1/2}.$$

Besides, for any piecewise constant p , let $[p]_e = p|_{T_e^+} - p|_{T_e^-}$ denote its jump on the side e , where T_e^+ and T_e^- are triangles sharing the common side e .

Furthermore, the stabilized finite element scheme seeks $(u_h, p_h) \in X_h \times M_h$ such that

$$(2.2) \quad \begin{cases} \sigma(u_h, v) + \nu(\nabla u_h, \nabla v) - (p_h, \operatorname{div} v) = f(v) & \forall v \in X_h, \\ (q, \operatorname{div} u) + S(p_h, q) = 0 & \forall q \in M_h. \end{cases}$$

According to [7], there exist a positive constant β_2 such that

$$\sup_{v_h \in X_h} \frac{\int_{\Omega} p_h \nabla \cdot v_h \, dx}{\|v_h\|_1} \geq \beta_2 \|p_h\| - C\|[p_h]_e\|_{S_h} \quad \forall p_h \in M_h.$$

3. THE RECOVERY-BASED ERROR ESTIMATOR

Let

$$\delta = \lambda \nabla u - pI,$$

and let its numerical approximation be

$$\delta_h = \lambda \nabla u_h - p_h I.$$

Here (u_h, p_h) is the approximation solution of (2.2), I denotes the (2×2) -identity matrix, and λ is a positive parameter. We remark that the parameter λ plays an important role in calculation and influences the effectiveness of the recovery-based estimator. Besides, when $\lambda = 1$, it becomes the one shown in [24].

Denote by N the vertices in τ_h , N_e the vertices of the side e and N_h the vertices in τ_h lying inside Ω . For any given $z \in N$, φ_z is the basis functions of z and the set $\omega_z := \text{supp } \varphi_z$, the union of all triangles sharing the same node z . Similarly to the method in [24], as a recovery technique, we need to construct $G(\delta_h)$ based on δ_h such that $G(\delta_h)$ approximates δ better than δ_h in some norm. Namely, $G(\delta_h)$ satisfies

$$\frac{\|\delta - G(\delta_h)\|}{\|\delta - \delta_h\|} \ll 1,$$

thus,

$$\frac{\|\delta_h - G(\delta_h)\|}{\|\delta - \delta_h\|} \approx 1.$$

The formulation of G actually can be written as

$$G(\delta_h)(z) = \frac{\int_{\omega_z} \delta_h \, dx}{\int_{\omega_z} 1 \, dx}.$$

Now, our recovery-based error estimator is constructed locally as

$$\eta_T := \|\delta_h - G(\delta_h)\|_T,$$

and the global one can be defined as

$$\eta := \left(\sum_{T \in \tau_h} \eta_T^2 \right)^{1/2}.$$

For any piecewise constant tensor δ , let $[\delta \cdot n_e] := \delta|_{T_e^+} \cdot n_e - \delta|_{T_e^-} \cdot n_e$ represent the jump of the normal component of δ on the edge $e \in S_h$, where n_e is the unit vector

and is orthogonal to e ; $[\delta \cdot \iota_e] := \delta|_{T_e^+} \cdot \iota_e - \delta|_{T_e^-} \cdot \iota_e$ represent the jump of the unit tangential vector ι_e of δ on the edge e . Next, we will give reliability and efficiency of the recovery-based error estimator. First, we need the following lemmas.

Lemma 3.1. *There exist two mesh-size-independent positive constants C_1 and C_2 such that*

$$C_1(\|[\delta_h \cdot n_e]\|_{S_h} + \|[p_h]_e\|_{S_h}) \leq \|\delta_h - G(\delta_h)\| \leq C_2(\|[\delta_h \cdot n_e]\|_{S_h} + \|[p_h]_e\|_{S_h}).$$

Proof. First, we have

$$(3.1) \quad C_1\|[\delta_h]_e\|_{S_h} \leq \|\delta_h - G(\delta_h)\| \leq C_2\|[\delta_h]_e\|_{S_h}.$$

We refer to Lemma 3.1 in [24] for its proof. Since $[\nabla u_h \cdot \iota_e] = 0$, we have

$$[\delta_h]_e = [\delta_h \cdot n_e]n_e + [\delta_h \cdot \iota_e]\iota_e = [\delta_h \cdot n_e]n_e + [-p_h I \cdot \iota_e]\iota_e.$$

Therefore, $\|[\delta_h]_e\|_e^2 = \|[\delta_h \cdot n_e]\|_e^2 + \|[p_h]_e\|_e^2$. Then together with (3.1), it admits $\|[p_h]_e\|_{S_h} \leq \|[\delta_h]_e\|_{S_h} \leq C\eta$, and this proves the left inequality of Lemma 3.1. For the right part,

$$(3.2) \quad \|[\delta_h]_e\|_{S_h} \leq C(\|[\delta_h \cdot n_e]\|_{S_h} + \|[p_h]_e\|_{S_h}).$$

Thus, the proof of Lemma 3.1 is complete. \square

Lemma 3.2 ([12], [24]). *There is a positive constant C such that*

$$\left\{ \sum_{e \in S_h} |h_e|^{-1} \|v - Q_h v\|_e^2 \right\}^{1/2} \leq C \|v\|_1 \quad \forall v \in X,$$

where $Q_h: L^1(\Omega)^2 \rightarrow X_h$ is a weighted Clément-type interpolation operator.

Lemma 3.3 ([12], [24]). *There is a positive constant C such that*

$$f(v - Q_h v) \leq CH_f \|v\|_1 \quad \forall v \in X,$$

where $H_f^2 = \sum_{z \in N/N_h} |\omega_z| \|f\|_{\omega_z}^2 + \sum_{z \in N_h} |\omega_z| \|f - \int_{\omega_z} f \, dx / \int_{\omega_z} 1 \, dx\|_{\omega_z}^2$. If $f \in L^2(\Omega)^2$, then the second term in H_f is a higher-order term. Besides, the first term is also a higher-order term for $f \in L^p(\Omega)^2$, $p > 2$.

Lemma 3.4. *For the projection stabilization term in (2.2), we have*

$$(q, \nabla \cdot u_h) \leq C\eta \|q\|.$$

Proof. Choosing $q = \nabla \cdot u_h$ in the second equation of (2.2) and using the properties of Π and the Schwarz inequality, we have

$$\begin{aligned} \|\nabla \cdot u_h\|^2 &= -S(p_h, \nabla \cdot u_h) = -(p_h - \Pi p_h, \nabla \cdot u_h - \Pi(\nabla \cdot u_h)) \\ &\leq \|p_h - \Pi p_h\| \|\nabla \cdot u_h - \Pi(\nabla \cdot u_h)\| \leq C\|[p_h]_e\|_{S_h} \|\nabla \cdot u_h\| \leq C\eta \|\nabla \cdot u_h\|. \end{aligned}$$

So, we arrive at

$$(q, \nabla \cdot u_h) \leq \|\nabla \cdot u_h\| \|q\| \leq C\eta \|q\|.$$

□

Theorem 3.1 (Reliability). *There exists a positive constant C independent of the mesh size such that*

$$\|(u - u_h, p - p_h)\| \leq C\beta_1^{-1}(H_f + \eta).$$

Proof. Choosing $v = Q_h v$ and $q = 0$ in (2.2) gives

$$B((u - u_h, p - p_h), (Q_h v, 0)) = 0 \quad \forall v \in X.$$

Noticing that if we only take $q = 0$ in (2.2), the term

$$\sigma(u - u_h, v) = -\nu(\nabla(u - u_h), \nabla v) + (p - p_h, \nabla \cdot v)$$

in the following can be replaced. Since $\nabla \cdot \delta_h|_T = 0$, by using integration by parts, we get

$$\begin{aligned} B((u - u_h, p - p_h), (v, q)) &= B((u - u_h, p - p_h), (v - Q_h v, q)) \\ &= \sigma(u - u_h, v - Q_h v) + \frac{\nu}{\lambda}(\lambda \nabla(u - u_h), \nabla(v - Q_h v)) \\ &\quad - \frac{\nu}{\lambda}(p - p_h, \nabla \cdot (v - Q_h v)) \\ &\quad - \left(1 - \frac{\nu}{\lambda}\right)(p - p_h, \nabla \cdot (v - Q_h v)) + (q, \nabla \cdot (u - u_h)) \end{aligned}$$

$$\begin{aligned}
&= \sigma(u - u_h, v - Q_h v) + \frac{\nu}{\lambda} ((\delta, \nabla(v - Q_h v))) + \frac{\nu}{\lambda} \sum_{T \in \tau_h} (\nabla \cdot \delta_h, v - Q_h v)_T \\
&\quad - \frac{\nu}{\lambda} \sum_{e \in S_h} ([\delta_h \cdot n_e], v - Q_h v)_e - \left(1 - \frac{\nu}{\lambda}\right) (p - p_h, \nabla \cdot (v - Q_h v)) - (q, \nabla \cdot u_h) \\
&= (f, v - Q_h v) - \sigma(u_h, v - Q_h v) + \left(1 - \frac{\nu}{\lambda}\right) \sum_{e \in S_h} ([p_h]_e, v - Q_h v)_e - (q, \nabla \cdot u_h) \\
&\quad - \frac{\nu}{\lambda} \sum_{e \in S_h} ([\delta_h \cdot n_e], v - Q_h v)_e \\
&\leq C \left((f, v - Q_h v) + \left(1 - \frac{\nu}{\lambda}\right) \sum_{e \in S_h} ([p_h]_e, v - Q_h v)_e \right. \\
&\quad \left. + \frac{\nu}{\lambda} \sum_{e \in S_h} ([\delta_h \cdot n_e], v - Q_h v)_e + (q, \nabla \cdot u_h) \right) = I_1 + I_2 + I_3 + I_4.
\end{aligned}$$

Moreover, by Lemma 3.3, it is easy to find that

$$I_1 \leq CH_f \|v\|_1.$$

Further, for I_2 , using the Schwarz inequality and Lemmas 3.2 and 3.1, we have

$$I_2 \leq C \left(1 - \frac{\nu}{\lambda}\right) \| [p_h]_e \|_{S_h} \left(\sum_{e \in S_h} h_e^{-1} \|v - Q_h v\|_e^2 \right)^{1/2} \leq C \left(1 - \frac{\nu}{\lambda}\right) \eta \|v\|_1.$$

Based on Lemmas 3.4, 3.1, and 3.2, we have

$$\begin{aligned}
I_3 &\leq C \frac{\nu}{\lambda} \| [\delta_h \cdot n_e] \|_{S_h} \left(\sum_{e \in S_h} h_e^{-1} \|v - Q_h v\|_e^2 \right)^{1/2} \leq C \frac{\nu}{\lambda} \eta \|v\|_1, \\
I_4 &\leq C \eta \|q\|.
\end{aligned}$$

Hence, from the above estimates, we deduce that

$$I_1 + I_2 + I_3 + I_4 \leq C (H_f + \eta) (\|v\|_1 + \|q\|).$$

Finally, we get

$$\begin{aligned}
\|(u - u_h, p - p_h)\| &\leq \beta_1^{-1} \sup_{(v, q) \in X \times M} \frac{B((u - u_h, p - p_h), (v, q))}{\|(v, q)\|} \\
&\leq C \beta_1^{-1} (H_f + \eta).
\end{aligned}$$

This completes the proof of reliability. \square

We now give a result about efficiency. From Lemma 3.1, we have

$$\eta \leq C(\|[\delta_h \cdot n_e]_e\|_{S_h} + \|[p_h]_e\|_{S_h}).$$

In the sequel we will give the estimation of the terms $\|[\delta_h \cdot n_e]_e\|_{S_h}$ and $\|[p_h]_e\|_{S_h}$.

According to [6], with every element T and every interior edge e we associate the element bubble function $\Phi_T = 27\Pi_{z \in N_T} \varphi_z$ and the edge bubble function $\Psi_e = 4\Pi_{z \in N_e} \varphi_z$, respectively. The following estimates are proved in Lemma 3.3 of [27]:

For an arbitrary polynomial q , one has

$$(3.3) \quad \|q\|_T \leq C\|\Phi_T^{1/2}q\|_T,$$

$$(3.4) \quad \|\nabla(q\Phi_T)\|_T \leq Ch_T^{-1}\|q\|_T,$$

$$(3.5) \quad \|q\|_e \leq C\|\Psi_e^{1/2}q\|_e,$$

$$(3.6) \quad \|\nabla(q\Psi_e)\|_T \leq Ch_e^{-1/2}\|q\|_e,$$

$$(3.7) \quad \|q\Psi_e\|_T \leq Ch_e^{1/2}\|q\|_e.$$

Lemma 3.5. *Let (u, p) and (u_h, p_h) be the solutions of (2.1) and (2.2), respectively. Then there exists a positive constant C independent of the mesh such that*

$$\|f_h + \nabla \cdot \delta_h - \sigma u_h\|_T \leq C(h_T^{-1}\|\delta - \delta_h\|_T + \|f_h - f\|_T + \sigma\|u - u_h\|_T),$$

where f_h is an approximation of f from the finite element space X_h .

Proof. Set $\zeta_T = \Phi_T(f_h + \nabla \cdot \delta_h - \sigma u_h)$. Using (3.3), (3.4), the Cauchy-Schwarz inequality, and integration by parts gives

$$\begin{aligned} \|f_h + \nabla \cdot \delta_h - \sigma u_h\|_T^2 &\leq C \int_T (f_h + \nabla \cdot \delta_h - \sigma u_h) \zeta_T \, dx \\ &\leq C \int_T (f_h - f) \zeta_T \, dx + \int_T (\delta - \delta_h) \nabla \zeta_T \, dx + \int_T \sigma (u - u_h) \zeta_T \, dx \\ &\leq C(h_T^{-1}\|\delta - \delta_h\|_T + \|f_h - f\|_T + \sigma\|u - u_h\|_T) \|f_h + \nabla \cdot \delta_h - \sigma u_h\|_T, \end{aligned}$$

and we arrive at the result. \square

Lemma 3.6. *Under the same assumption as in Lemma 3.5, we have*

$$\|[\delta_h \cdot n_e]\|_{S_h} \leq C(h\|f - f_h\| + h\|u - u_h\| + \|\delta - \delta_h\|).$$

Proof. Set $\theta_e = \Psi_e[\delta_h \cdot n_e]$. Then, utilizing the properties of (3.5), (3.6), (3.7), Lemma 3.5, the Cauchy-Schwarz inequality, and integration by parts, we obtain

$$\begin{aligned}
\|[\delta_h \cdot n_e]\|_e^2 &\leq C \int_e [\delta_h \cdot n_e] \theta_e \, dx \leq C \sum_{i=1}^2 \left(\int_{T_i} (f - \sigma u) \theta_e - (\delta - \delta_h) \nabla \theta_e \, dx \right) \\
&= C \sum_{i=1}^2 \left(\int_{T_i} (f - f_h + f_h - \sigma u_h + \sigma u_h - \sigma u) \theta_e - (\delta - \delta_h) \nabla \theta_e \, dx \right) \\
&\leq C [h_e^{1/2} (\|f - f_h\|_{\omega_e} + \|f_h + \nabla \cdot \delta_h - \sigma u_h\|_{\omega_e} + \sigma \|u - u_h\|_{\omega_e})] \|[\delta_h \cdot n_e]\|_e \\
&\quad + C h_e^{-1/2} \|\delta - \delta_h\|_{\omega_e} \|[\delta_h \cdot n_e]\|_e \\
&\leq C (h_e^{1/2} (\|f - f_h\|_{\omega_e} + \sigma \|u - u_h\|_{\omega_e}) + h_e^{-1/2} \|\delta - \delta_h\|_{\omega_e}) \|[\delta_h \cdot n_e]\|_e.
\end{aligned}$$

Immediately,

$$\|[\delta_h \cdot n_e]\|_{S_h} = \sum_{e \in S_h} h_e^{1/2} \|[\delta_h \cdot n_e]\| \leq C (h \|f - f_h\| + h \|u - u_h\| + \|\delta - \delta_h\|).$$

For the term $\|[p_h]_e\|_{S_h}$, the estimate is the same as in Lemmas 3.4 and 3.5 in [24] and we have

$$(3.8) \quad \|[p_h]_e\|_{S_h} \leq C \|(u - u_h, p - p_h)\|.$$

□

Theorem 3.2 (Efficiency). *Let (u, p) and (u_h, p_h) be the solutions of (2.1) and (2.2), respectively. There exists a positive constant C independent of the mesh size such that*

$$\eta \leq C \left(\|(u - u_h, p - p_h)\| + h \|u - u_h\| + \sum_{e \in S_h} h_e \inf_{f_h \in X_h} \|f - f_h\|_{\omega_e} \right).$$

Proof. Using Lemmas 3.5, 3.6 and (3.8), we get

$$\begin{aligned}
\eta &\leq C (\|[\delta_h \cdot n_e]\|_{S_h} + \|[p_h]_e\|_{S_h}) \\
&\leq C \left(\|\delta - \delta_h\| + \sum_{e \in S_h} h_e \inf_{f_h \in X_h} \|f - f_h\|_{\omega_e} + h \|u - u_h\| + \|(u - u_h, p - p_h)\| \right) \\
&\leq C \left(\|(u - u_h, p - p_h)\| + h \|u - u_h\| + \sum_{e \in S_h} h_e \inf_{f_h \in X_h} \|f - f_h\|_{\omega_e} \right).
\end{aligned}$$

□

4. NUMERICAL EXPERIMENTS

In this section, we focus on the performance of the recovery-based estimator described in former sections. First we introduce the strategy of refinement of the mesh. Note that the mesh is updated by adding some new nodes and the mesh modification requires the regularity of the mesh.

Step 1. Calculate the initial numerical solution in the initial mesh h_j .

Step 2. For every element, calculate the local error estimator η_T , and then compute the average $\bar{\eta} = \sum_T \eta_T / \sum_T 1$ in all the elements of the presented mesh.

Step 3. Define the intermediate function $g = \min(\max(\eta_T / (c\bar{\eta}), 1.0), 3.0)$, commonly the constant $0 < c < 1$. Use the intermediate function g to update the size of mesh

$$h_{j+1} = h_j / g(\bar{\eta}),$$

and then get a new mesh and return to step 1 unless $j < M$ (M is the number of refinement).

For convenience, we need the following notions.

- ▷ Dof_j is the number of the triangles for the triangulation with the mesh size h_j ;
- ▷ $e_r^j = \|(u - u_h^j, p - p_h^j)\| / \|(u, p)\|$ is the relative error in the energy norm;
- ▷

$$\text{Order}_1 = 2 \frac{\log(e_r^{j+1}) - \log(e_r^j)}{\log(\text{Dof}_j / \text{Dof}_{j+1})}$$

is the convergence rate of the error e_r^j ;

- ▷ $\eta_r^j = \eta / \|(\lambda u, p)\|$ is the relative value of η ;
- ▷

$$\text{Order}_2 = 2 \frac{\log(\eta_r^{j+1}) - \log(\eta_r^j)}{\log(\text{Dof}_j / \text{Dof}_{j+1})}$$

is the convergence rate of η_r^j ;

- ▷ $E = \eta_r^j / e_r^j$ is the effective index of the recovery-based estimator η .

4.1. Analytical solution on square domain. For the first example, we use as domain the square $\Omega = (0, 1) \times (0, 1)$ and set f to be such that the exact solution of our problem (1.1) is given by

$$\begin{aligned} u_1(x, y) &= -256x^2(x-1)^2y(y-1)(2y-1), \\ u_2(x, y) &= 256y^2(y-1)^2x(x-1)(2x-1), \\ p(x, y) &= 150(x-0.5)(y-0.5). \end{aligned}$$

First, we report the case in which we have considered the values $\nu = 10^{-6}$ and $\sigma = 1$ with different values of λ . The results are contained in Tables 1–4. From these

tables, we can see that, except $\lambda = 1$ (the case of estimator in [24]), the recovery-based estimator works well and gets nearly optimal convergence order. In addition, the effectivity index E approaches 1.0, which illustrates the recovery-based estimator performs well. Thus, it is concluded that if we choose very small value of λ then we can get good numerical results.

Level	Dof _{<i>j</i>}	e_r^j	Order ₁	η_r	Order ₂	E
0	162	0.3191	–	0.1974	–	0.6185
1	226	0.2676	1.0562	0.1780	0.6193	0.6652
2	381	0.2280	0.6137	0.1729	0.1123	0.7582
3	629	0.2001	0.5201	0.1363	0.9486	0.6810
4	1014	0.1751	0.5597	0.1252	0.3567	0.7148

Table 1. Numerical results based on $\nu = 10^{-6}$, $\sigma = 1$, and $\lambda = 1$.

Level	Dof _{<i>j</i>}	e_r^j	Order ₁	η_r	Order ₂	E
0	162	0.1798	–	0.1848	–	1.0280
1	261	0.1471	0.8428	0.1479	0.9336	1.0060
2	432	0.1118	1.0870	0.1121	1.1006	1.0025
3	699	0.0882	0.9852	0.0873	1.0376	0.9900
4	1110	0.0698	1.0111	0.0689	1.0269	0.9863

Table 2. Numerical results based on $\nu = 10^{-6}$, $\sigma = 1$, and $\lambda = 10^{-1}$.

Level	Dof _{<i>j</i>}	e_r^j	Order ₁	η_r	Order ₂	E
0	162	0.1790	–	0.1863	–	1.0406
1	263	0.1467	0.8215	0.1487	0.9312	1.0133
2	442	0.1097	1.1220	0.1110	1.1269	1.0120
3	707	0.0865	1.0101	0.0870	1.0371	1.0057
4	1084	0.0692	1.0467	0.0694	1.0593	1.0029

Table 3. Numerical results based on $\nu = 10^{-6}$, $\sigma = 1$, and $\lambda = 10^{-2}$.

Level	Dof _{<i>j</i>}	e_r^j	Order ₁	η_r	Order ₂	E
0	162	0.1792	–	0.1865	–	1.0406
1	263	0.1469	0.8215	0.1488	0.9311	1.0133
2	434	0.1106	1.1326	0.1120	1.1338	1.0130
3	717	0.0863	0.9895	0.0868	1.0165	1.0062
4	1124	0.0669	1.1341	0.0671	1.1421	1.0044

Table 4. Numerical results based on $\nu = 10^{-6}$, $\sigma = 1$, and $\lambda = 10^{-3}$.

Further, we consider the cases $\lambda = 10^{-3}$ with different values of ν and σ . In Tables 4–6, we show the evolution of the finite element errors when σ grows. Besides, in Tables 6–8, we report numerical errors and effectivity indices with small values of ν . From all the results in Tables 4–8, we can observe that the recovery-based error estimator with a small value of λ works well for the $P_1 - P_0$ stabilized method.

Level	Dof _{<i>j</i>}	e_r^j	Order ₁	η_r	Order ₂	E
0	162	0.1989	–	0.2024	–	1.0176
1	278	0.1481	1.0914	0.1473	1.1765	0.9945
2	464	0.1093	1.1858	0.1097	1.1524	1.0030
3	714	0.0866	1.0841	0.0865	1.1025	0.9991
4	1091	0.0699	1.0069	0.0697	1.0181	0.9967

Table 5. Numerical results based on $\nu = 10^{-6}$, $\sigma = 10$, and $\lambda = 10^{-3}$.

Level	Dof _{<i>j</i>}	e_r^j	Order ₁	η_r	Order ₂	E
0	162	0.2351	–	0.2014	–	0.8566
1	277	0.1715	1.1745	0.1451	1.2207	0.8461
2	454	0.1225	1.3635	0.1114	1.0714	0.9094
3	695	0.0955	1.1694	0.0887	1.0721	0.9284
4	1024	0.0764	1.1539	0.0715	1.1076	0.9368

Table 6. Numerical results based on $\nu = 10^{-6}$, $\sigma = 100$, and $\lambda = 10^{-3}$.

Level	Dof _{<i>j</i>}	e_r^j	Order ₁	η_r	Order ₂	E
0	162	0.2351	–	0.2014	–	0.8566
1	277	0.1715	1.1745	0.1451	1.2207	0.8461
2	456	0.1232	1.3294	0.1117	1.0493	0.9072
3	695	0.0964	1.1647	0.0892	1.0718	0.9252
4	1069	0.0757	1.1233	0.0711	1.0486	0.9402

Table 7. Numerical results based on $\nu = 10^{-4}$, $\sigma = 100$, and $\lambda = 10^{-3}$.

Level	Dof _{<i>j</i>}	e_r^j	Order ₁	η_r	Order ₂	E
0	162	0.2357	–	0.2013	–	0.8540
1	279	0.1739	1.1184	0.1457	1.1876	0.8380
2	453	0.1234	1.4152	0.1131	1.0475	0.9162
3	718	0.0966	1.0625	0.0892	1.0306	0.9229
4	1164	0.0734	1.1372	0.0692	1.0482	0.9430

Table 8. Numerical results based on $\nu = 10^{-2}$, $\sigma = 100$, and $\lambda = 10^{-3}$.

Finally, Figure 1 plots the uniform mesh without the adaptive method having 1624 triangle elements and the adaptive mesh with the recovery-based estimator with 1698 triangle elements. We can find that using almost the same number of elements the distribution of the adaptive mesh is more reasonably based on the exact solution and domain.

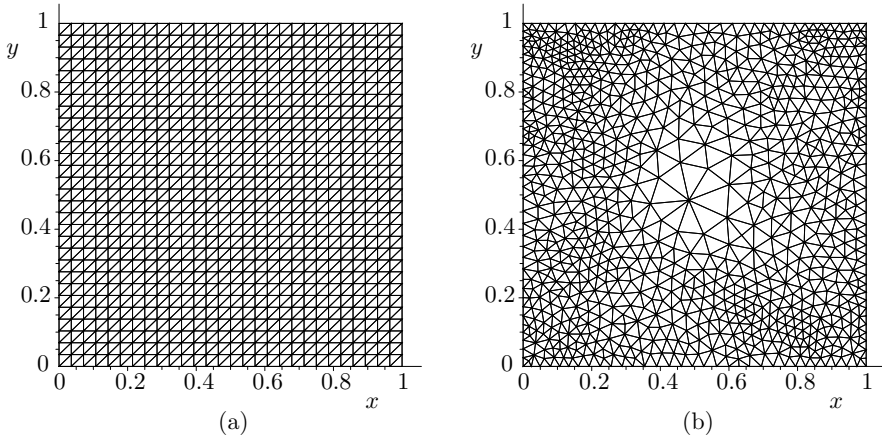


Figure 1. (a) uniform mesh with 1624 elements and (b) adaptive mesh with 1698 elements.

4.2. Analytical solution on L-shape domain. We consider the following numerical test on the L-shape domain $\Omega = (-1, 1)^2 - [0, 1]^2$ with a smooth solution

$$\begin{aligned}
 u_1(x, y) &= \frac{y - 0.1}{\sqrt{(x - 0.1)^2 + (y - 0.1)^2}}, \\
 u_2(x, y) &= -\frac{x - 0.1}{\sqrt{(x - 0.1)^2 + (y - 0.1)^2}}, \\
 p(x, y) &= \frac{1}{y + 1.05} - \frac{\log(2.05) + \log(1.05) - 2 \log(0.05)}{3}.
 \end{aligned}$$

Note that this domain Ω is a non-convex domain.

In Figure 2, we draw the initial mesh and the refined mesh with the recovery-based error estimator. We note that in the singular place the mesh is very dense using the strategy of refinement of the mesh. Next, in Figure 3 we show relative errors in energy norm about e_r and η_r with $\nu = 10^{-6}$, $\sigma = 1$, and four values of λ . From the figure we can see that the relative error decreases in energy norm based on the adaptive refinements and the value of the estimator η_r is very close to the true error e_r when the value of λ becomes small, which illustrates the recovery-based estimator works well for the $P_1 - P_0$ stabilized method. From Figure 3(a), we also note that the value of the recovery-based estimator in [24], i.e., $\lambda = 1$, is not close to the true error, though the relative error becomes small.

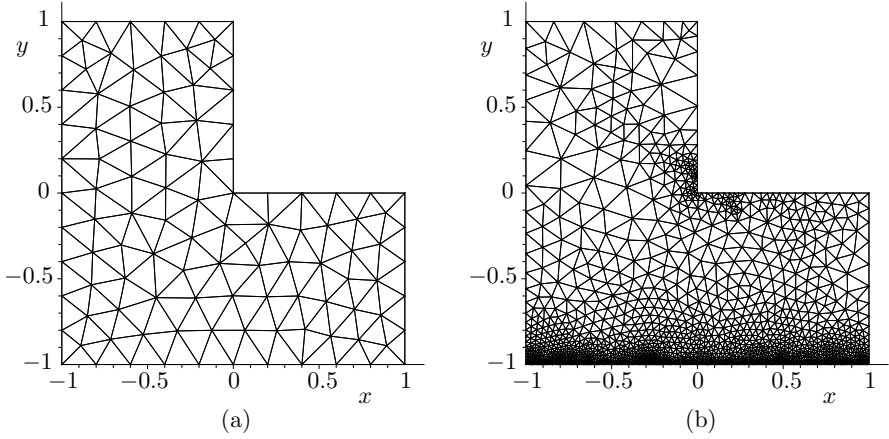


Figure 2. (a) the initial mesh and (b) the refined mesh.

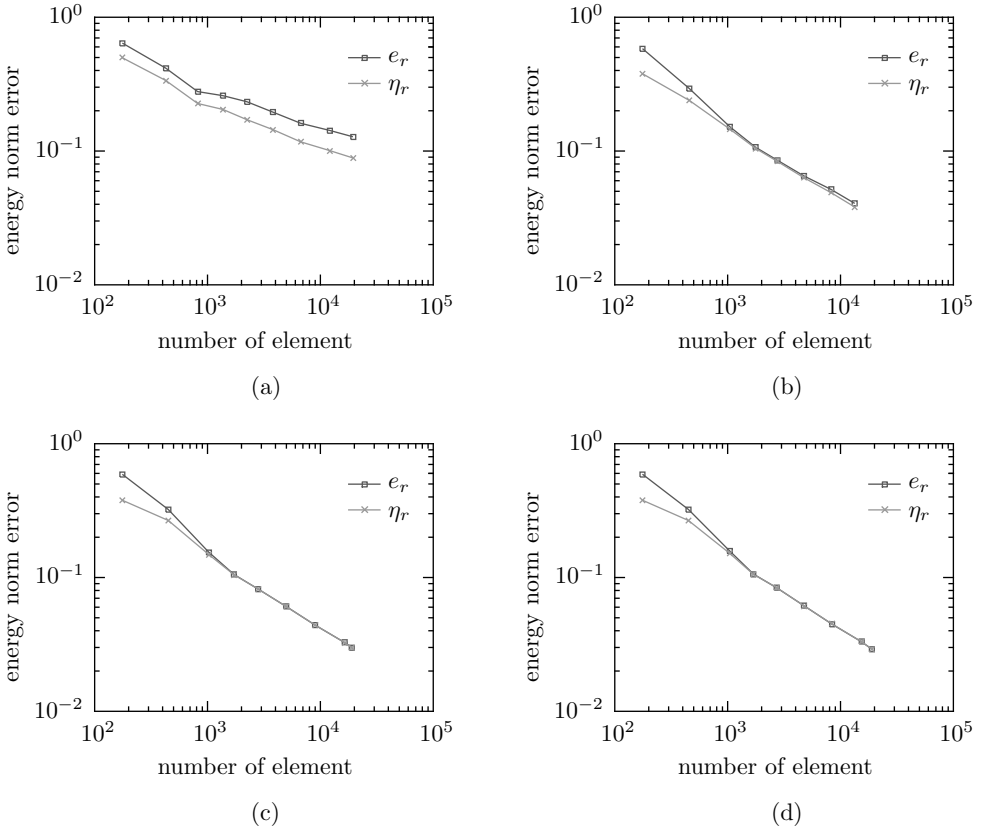


Figure 3. Relative errors in energy norm with (a) $\lambda = 1$, (b) $\lambda = 10^{-1}$, (c) $\lambda = 10^{-2}$, and (d) $\lambda = 10^{-3}$.

From the above test, we find that when λ is taken close to the value 10^{-2} , the recovery-based estimator converges better. Thus, in the following tests, we focus on the different values of ν and σ based on $\lambda = 10^{-2}$. Tables 9–11 show that when the value of σ increases, the effectivity index of the recovery-based estimator is weaker for small viscosity coefficient $\nu = 10^{-6}$ although the relative error in energy norm becomes small. However, from Tables 9 and 12–13, we can see that when the value of viscosity changes from 10^{-4} to 10^{-8} and $\sigma = 1$, the effectivity index of the recovery-based estimator is nearly stable and close to 1.

Level	Dof _{<i>j</i>}	e_r^j	Order ₁	η_r	Order ₂	E
0	176	0.5906	–	0.3779	–	0.6400
1	449	0.3225	1.2920	0.2669	0.7431	0.8275
2	1028	0.1543	1.7794	0.1483	1.4180	0.9611
3	1719	0.1053	1.4870	0.1048	1.3516	0.9952
4	2792	0.0822	1.0201	0.0823	0.9964	1.0009

Table 9. Numerical results based on $\nu = 10^{-6}$, $\sigma = 1$, and $\lambda = 10^{-2}$.

Level	Dof _{<i>j</i>}	e_r^j	Order ₁	η_r	Order ₂	E
0	176	0.5983	–	0.3682	–	0.6154
1	457	0.3259	1.2731	0.2669	0.6746	0.8188
2	1061	0.1526	1.8013	0.1436	1.4715	0.9408
3	1762	0.1055	1.4563	0.1042	1.2662	0.9872
4	2971	0.0828	0.9290	0.0824	0.8980	0.9952

Table 10. Numerical results based on $\nu = 10^{-6}$, $\sigma = 10$, and $\lambda = 10^{-2}$.

Level	Dof _{<i>j</i>}	e_r^j	Order ₁	η_r	Order ₂	E
0	176	0.6869	–	0.3336	–	0.4857
1	469	0.3660	1.2850	0.2362	0.7050	0.6454
2	1106	0.2164	1.2243	0.1372	1.2665	0.6338
3	1858	0.1669	1.0024	0.1061	0.9909	0.6357
4	2960	0.1158	1.5685	0.0843	0.9870	0.7279

Table 11. Numerical results based on $\nu = 10^{-6}$, $\sigma = 100$, and $\lambda = 10^{-2}$.

Level	Dof _{<i>j</i>}	e_r^j	Order ₁	η_r	Order ₂	E
0	176	0.5906	–	0.3779	–	0.6399
1	449	0.3225	1.2918	0.2669	0.7429	0.8274
2	1030	0.1525	1.8050	0.1467	1.4411	0.9624
3	1714	0.1060	1.4289	0.1057	1.2884	0.9974
4	2672	0.0825	1.1259	0.0827	1.1033	1.0025

Table 12. Numerical results based on $\nu = 10^{-4}$, $\sigma = 1$, and $\lambda = 10^{-2}$.

Level	Dof _j	e_r^j	Order ₁	η_r	Order ₂	E
0	176	0.5905	–	0.3779	–	0.6400
1	447	0.3217	1.3032	0.2686	0.7330	0.8348
2	1014	0.1559	1.7690	0.1499	1.4242	0.9614
3	1687	0.1037	1.6031	0.1032	1.4658	0.9956
4	2883	0.0793	1.0009	0.0795	0.9737	1.0029

Table 13. Numerical results based on $\nu = 10^{-8}$, $\sigma = 1$, and $\lambda = 10^{-2}$.



It should be noticed that in practice the recovery-based estimator is efficient for this singular problem with small viscosity and reaction coefficient or large viscosity and reaction coefficient. We remark that for small viscosity and large reaction coefficient, our recovery-based estimator needs to be established for another stabilized method, such as the stabilized method in [15].

Acknowledgements. The authors would like to thank the editor and reviewers for their valuable comments and suggestions which helped us to improve the quality of this paper.

References

- [1] *R. Araya, G. R. Barrenechea, A. Poza*: An adaptive stabilized finite element method for the generalized Stokes problem. *J. Comput. Appl. Math.* *214* (2008), 457–479. [zbl](#) [MR](#) [doi](#)
- [2] *I. Babuška, W. C. Rheinboldt*: A-posteriori error estimates for the finite element method. *Int. J. Numer. Methods Eng.* *12* (1978), 1597–1615. [zbl](#) [doi](#)
- [3] *R. E. Bank, B. D. Welfert*: A comparison between the mini-element and the Petrov-Galerkin formulations for the generalized Stokes problem. *Comput. Methods Appl. Mech. Eng.* *83* (1990), 61–68. [zbl](#) [MR](#) [doi](#)
- [4] *G. R. Barrenechea, F. Valentin*: An unusual stabilized finite element method for a generalized Stokes problem. *Numer. Math.* *92* (2002), 653–677. [zbl](#) [MR](#) [doi](#)
- [5] *T. P. Barrios, R. Bustinza, G. C. García, E. Hernández*: On stabilized mixed methods for generalized Stokes problem based on the velocity-pseudostress formulation: A priori error estimates. *Comput. Methods Appl. Mech. Eng.* *237–240* (2012), 78–87. [zbl](#) [MR](#) [doi](#)
- [6] *C. Bernardi, R. Verfürth*: Adaptive finite element methods for elliptic equations with non-smooth coefficients. *Numer. Math.* *85* (2000), 579–608. [zbl](#) [MR](#) [doi](#)
- [7] *P. B. Bochev, C. R. Dohrmann, M. D. Gunzburger*: Stabilization of low-order mixed finite elements for the Stokes equations. *SIAM J. Numer. Anal.* *44* (2006), 82–101. [zbl](#) [MR](#) [doi](#)
- [8] *E. Burman, P. Hansbo*: Edge stabilization for the generalized Stokes problem: A continuous interior penalty method. *Comput. Methods Appl. Mech. Eng.* *195* (2006), 2393–2410. [zbl](#) [MR](#) [doi](#)
- [9] *R. Bustinza, G. N. Gatica, M. González*: A mixed finite element method for the generalized Stokes problem. *Int. J. Numer. Methods Fluids* *49* (2005), 877–903. [zbl](#) [MR](#) [doi](#)
- [10] *C. Carstensen*: Some remarks on the history and future of averaging techniques in a posteriori finite element error analysis. *ZAMM, Z. Angew. Math. Mech.* *84* (2004), 3–21. [zbl](#) [MR](#) [doi](#)

- [11] *C. Carstensen, S. A. Funken*: A posteriori error control in low-order finite element discretisations of incompressible stationary flow problems. *Math. Comput.* *70* (2001), 1353–1381. [zbl](#) [MR](#) [doi](#)
- [12] *C. Carstensen, R. Verfürth*: Edge residuals dominate a posteriori error estimates for low order finite element methods. *SIAM J. Numer. Anal.* *36* (1999), 1571–1587. [zbl](#) [MR](#) [doi](#)
- [13] *S. H. Chou*: Analysis and convergence of a covolume method for the generalized Stokes problem. *Math. Comput.* *66* (1997), 85–104. [zbl](#) [MR](#) [doi](#)
- [14] *Q. Deng, X. Feng*: Multigrid methods for the generalized Stokes equations based on mixed finite element methods. *J. Comput. Math.* *20* (2002), 129–152. [zbl](#) [MR](#)
- [15] *H.-Y. Duan, P.-W. Hsieh, R. C. E. Tan, S.-Y. Yang*: Analysis of the small viscosity and large reaction coefficient in the computation of the generalized Stokes problem by a novel stabilized finite element method. *Comput. Methods Appl. Mech. Eng.* *271* (2014), 23–47. [zbl](#) [MR](#) [doi](#)
- [16] *C. A. Duarte, J. T. Oden*: An h - p adaptive method using clouds. *Comput. Methods Appl. Mech. Eng.* *139* (1996), 237–262. [zbl](#) [MR](#) [doi](#)
- [17] *Y. He, C. Xie, H. Zheng*: A posteriori error estimate for stabilized low-order mixed FEM for the Stokes equations. *Adv. Appl. Math. Mech.* *2* (2010), 798–809. [zbl](#) [MR](#) [doi](#)
- [18] *P. Huang, Q. Zhang*: A posteriori error estimates for the Stokes eigenvalue problem based on a recovery type estimator. *Bull. Math. Soc. Sci. Math. Répub. Soc. Roum., Nouv. Sér.* *62* (2019), 295–304. [MR](#)
- [19] *D. Kay, D. Silvester*: A posteriori error estimation for stabilized mixed approximations of the Stokes equations. *SIAM J. Sci. Comput.* *21* (1999), 1321–1336. [zbl](#) [MR](#) [doi](#)
- [20] *M. Larin, A. Reusken*: A comparative study of efficient iterative solvers for generalized Stokes equations. *Numer. Linear Algebra Appl.* *15* (2008), 13–34. [zbl](#) [MR](#) [doi](#)
- [21] *K. Nafa, A. J. Wathen*: Local projection stabilized Galerkin approximations for the generalized Stokes problem. *Comput. Methods Appl. Mech. Eng.* *198* (2009), 877–883. [zbl](#) [MR](#) [doi](#)
- [22] *S. Repin, R. Stenberg*: A posteriori error estimates for the generalized Stokes problem. *J. Math. Sci., New York* *142* (2007), 1828–1843; translation from *Probl. Mat. Anal.* *34* (2006), 89–101. [zbl](#) [MR](#) [doi](#)
- [23] *R. Rodríguez*: Some remarks on Zienkiewicz-Zhu estimator. *Numer. Methods Partial Differ. Equations* *10* (1994), 625–635. [zbl](#) [MR](#) [doi](#)
- [24] *L. Song, Y. Hou, Z. Cai*: Recovery-based error estimator for stabilized finite element methods for the Stokes equation. *Comput. Methods Appl. Mech. Eng.* *272* (2014), 1–16. [zbl](#) [MR](#) [doi](#)
- [25] *R. Verfürth*: A posteriori error estimators for the Stokes equations. *Numer. Math.* *55* (1989), 309–325. [zbl](#) [MR](#) [doi](#)
- [26] *R. Verfürth*: A posteriori error estimates for nonlinear problems: Finite element discretizations of elliptic equations. *Math. Comput.* *62* (1994), 445–475. [zbl](#) [MR](#) [doi](#)
- [27] *R. Verfürth*: A Review of A Posteriori Error Estimation and Adaptive Mesh-Refinement Techniques. Wiley-Teubner Series Advances in Numerical Mathematics, Wiley, Chichester; Teubner, Stuttgart, 1996. [zbl](#)
- [28] *Z. Wang, Z. Chen, J. Li*: A stabilized nonconforming quadrilateral finite element method for the generalized Stokes equations. *Int. J. Numer. Anal. Model.* *9* (2012), 449–457. [zbl](#) [MR](#)
- [29] *J. Wang, Y. Wang, X. Ye*: A posteriori error estimate for stabilized finite element methods for the Stokes equations. *Int. J. Numer. Anal. Model.* *9* (2012), 1–16. [zbl](#) [MR](#)
- [30] *H. Zheng, Y. Hou, F. Shi*: A posteriori error estimates of stabilization of low-order mixed finite elements for incompressible flow. *SIAM J. Sci. Comput.* *32* (2010), 1346–1360. [zbl](#) [MR](#) [doi](#)
- [31] *O. C. Zienkiewicz, J. Z. Zhu*: The superconvergent patch recovery and a posteriori error estimates. I: The recovery technique. *Int. J. Numer. Methods Eng.* *33* (1992), 1331–1364. [zbl](#) [MR](#) [doi](#)

- [32] *O. C. Zienkiewicz, J. Z. Zhu*: Superconvergence and the superconvergent patch recovery. *Finite Elem. Anal. Des.* 19 (1995), 11–23.  

Authors' addresses: Pengzhan Huang (corresponding author), College of Mathematics and System Sciences, Xinjiang University, Urumqi 830046, P. R. China, e-mail: hpzh007@yahoo.com, Qiyu Zhang, School of Mathematics and Statistics, Wuhan University, Wuhan 430072, P. R. China, e-mail: twinklerain@163.com.